RSC Advances

ROYAL SOCIETY OF CHEMISTRY

www.rsc.org/advances

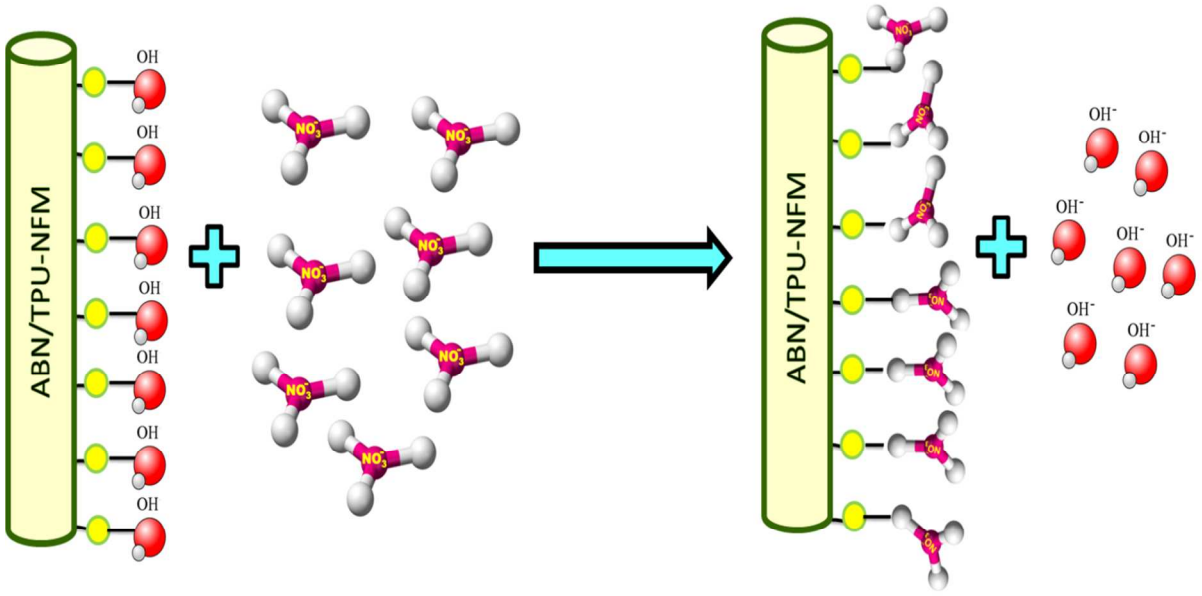

Nitrate scavenging by hybrid Al_2O_3/bio-TiO_2 nanocomposite impregnated thermoplastic polyurethane nanofibrous membrane

Journal Name

RSCPublishing

ARTICLE

Scavenging of nitrate ions from water using hybrid Al_2O_3/bio-TiO_2 nanocomposite impregnated thermoplastic polyurethane nanofibrous membrane

Cite this: DOI: 10.1039/x0xx00000x

Received 00th January 2012,
Accepted 00th January 2012

DOI: 10.1039/x0xx00000x

www.rsc.org/

S. P. Suriyaraj[a], Mamatha M. Pillai[b], Amitava Bhattacharyya[c], R. Selvakumar[a,b]*

In the present study, we have exploited the nitrate adsorption property of Al_2O_3/bio-TiO_2 nanocomposite (ABN) and ABN impregnated electrospun thermoplastic polyurethane nanofibrous membrane (ABN/TPU-NFM) for water purification. Nitrate adsorption was investigated both in batch and dip mode studies. Parameters like effect of contact time, adsorbate concentration and membrane size were optimized. The adsorption capacity (Q_0) of the ABN and ABN/TPU-NFM was found to be 30.3 and 14.9 mg/g, respectively. Kinetics of the adsorption process was studied using pseudo-first-order and second-order models and it was found to obey pseudo-second-order kinetic model. The phase identification, crystalline stability and the surface functional groups of the adsorbents involved in nitrate adsorption were characterized by X-ray diffraction (XRD) and Fourier transform infra-red (FTIR) spectroscopy. Leachability studies carried out using atomic absorption spectroscopy (AAS) indicated no leaching of impregnated nanoparticles from ABN/TPU-NFM in the treated water. No significant cytotoxicity for ABN was observed when tested with mouse fibroblast cells (L929), suggesting that the developed hybrid adsorbent is biocompatible and safe for drinking water purification. Further, field trial was carried out using natural ground water sample collected from nitrate contaminant area and tested for nitrate removal by dip mode adsorption process using ABN/TPU-NFM. The treated water was found to be potable having permissible limit of nitrate. This facile approach of designing nanocomposite impregnated nanofiber membrane is efficient in removing nitrate from contaminated drinking water.

1. Introduction

Nitrate contamination of drinking water is a major problem in developing countries.[1] In India, states like Andra Pradesh, Madhya Pradesh, Rajasthan and Tamil Nadu have been reported to have major nitrate pollution.[2] Consumption of water that has excessive nitrate can cause detrimental health impacts on human beings and leads to gastric cancer, goitre, birth defects, hypertension and methemoglobinemia.[3,4] Due to these clinical manifestations caused by nitrate contaminated drinking water, World Health Organization (WHO) has recommended 50 mg/L as the maximum contaminant level (MCL) in drinking water for nitrate.[5] Various methods like chemical precipitation[6], electrocoagulation[7], photocatalysis[2], reverse osmosis[8] and electrodialysis[9] have been reported to remove nitrate from drinking water.

Scientific evidences recommend adsorption as the most efficient and cost effective method to remove nitrate like ions when compared to other methods.[8,10] However, increasing concentration of nitrate in potable water due to natural and anthropogenic reasons warrants development of new materials that can efficiently remove nitrate and is also less toxic to the environment and to the consumers. Various adsorbent materials like ion exchange resins, activated carbon, metal oxides, nanocomposites, nanofibers, graphene, zeolites and hydroxyapatite have been investigated for their application in nitrate removal systems.[9,10] [11,12] Among the above adsorbent materials, the nanocomposite material has high efficiency to adsorb nitrate from aqueous solution than the individual nanoparticles or materials. Various nanocomposite materials like Mg-Al, Mg-Fe, Ca-Al, Pd/TiO_2, Cu/TiO_2, Au/TiO_2, Pd-Cu/Al_2O_3, Pd-Sn/Al_2O_3, Pd-In/Al_2O_3, Pd-Cu/TiO_2, Rh–Cu/Al_2O_3 have also been reported for the removal of nitrate.[13-21] However, only photocatalytic reduction was reported with these materials and the performances were not systematically compared to the conventional adsorption processes. These composite materials need external UV light energy and multifarious reaction chambers to perform nitrate removal and are said to produce toxic by products during the reaction.[22] Therefore, there is a vital need for affordable, sustainable, eco-

friendly and non toxic nanocomposite for the efficient adsorption of nitrate from contaminated water.

The inability to recover nanomaterials after adsorption process is still a setback. Such particle recovery or zero recovery ultimately lead to toxicological issue and add cost to the technology. In order to overcome these problems, the nanoparticles impregnated hybrid nanofibers have been researched for the removal of ionic pollutants in order to make them suitable for water treatment.[23,24] However, there are very few reports on the nanoparticle based nanofiber membranes for nitrate removal.[2] The main focus of the present study was to investigate the nitrate adsorption phenomena onto the developed ABN and ABN/TPU-NFM adsorbents. As per our knowledge, this is the first report, were the nitrate adsorption property of the hybrid adsorbent was exploited in both batch and dip mode experiments with aqueous solution and natural ground water. The experimental data were fitted onto suitable isotherm and kinetic models. The leachability and the toxicity studies were performed to support the possibility of using such composite nanofibrous membrane for treatment of drinking water.

2. Materials and method

2.1. Materials

All the chemicals used were of analytical grade. Titanium isopropoxide and aluminum hydroxide (purity > 99.9%) were purchased from Sigma Aldrich, India. N, N-dimethylformamide, tetraethyl orthosilicate (TEOS) and (3-Aminopropyl) triethoxysilane (APTES) were purchased from Merck, India. 3-(4,5-dimethylthiozol-2-yl)-2,5-diphenyl tetrazolium bromide (MTT), Dulbecco's Modified Eagle Medium (DMEM) and fetal bovine serum (FBS) were purchased from Himedia, India. Texin 945 U grade TPU was kindly donated by Bayer Material Science. Standard nitrate solution (Thermo Scientific, USA) was used as the model pollutant. Double distilled water was used throughout the experiment.

2.2. Preparation of ABN and ABN/TPU-NFM

The preparation of ABN and ABN/TPU-NFM was carried out according to the optimised method reported in our previous studies.[24] In brief, TiO_2 nanoparticles were synthesized using *Bacillus licheniformis*[25] and subsequently modified with an aluminum precursor to produce ABN and calcined at 700° C[25]. This hybrid nanocomposite material was impregnated on to the electrospun nanofiber using silane functionalization of both the fiber and the nanocomposite surfaces.[24]

2.3. Estimation of nitrate

Nitrate estimation was performed using Thermo Scientific Orion four star ion selective electrode meter, USA, according to EPA 9210 A standards.[26] The electrode was calibrated using standard nitrate concentrations in the range of 1–1000 mg/L. 1 mg/L was set as the minimum detection limit. Nitrate ionic strength adjustment buffer was used in estimation throughout the experiment.

2.4. Adsorption studies

The synthesized ABN and ABN/TPU-NFM were used as adsorbent materials for the removal of nitrate from aqueous solution. Experiments were conducted by simple batch mode adsorption for the ABN and dip mode adsorption method for ABN/TPU-NFM. Batch mode studies were carried out at room temperature by agitating 0.2 g of ABN in 200 mL of nitrate solution of desired concentrations and pH at 120 rpm. The flasks were withdrawn at predetermined time intervals and the adsorbate concentration in the supernatant was determined. In case of ABN/TPU-NFM, the experiments were carried out using simple dip mode adsorption method. Various concentrations of the adsorbate (25–125 mg/L of NO_3^-, respectively) were taken in flasks and dipped with 8x8 cm^2/200 mL of membrane material. The samples were withdrawn at pre-determined time intervals and estimated. The composite nanofibrous membrane was cut in to different square sizes of 2, 4, 6, 8 and 10 cm length and the studies were carried out in 200 mL of NO_3^- solution of desired concentration and pH at room temperature.

The adsorption percentage was determined using Equation 1.

$$\text{Percentage } NO_3^- \text{ removal} = (C_i - C_f)/ C_i \times 100 \quad (1)$$

Where C_i is the initial adsorbate concentration and C_f is final adsorbate concentration. The adsorption kinetics (Pseudo first order and second order) and Langmuir isotherm were employed to study the adsorption efficiency.

2.5. Characterization

The thickness measurement of the developed nanofiber membrane was carried out using digital fabric thickness gauge (DFTG, India) according to ASTM D1777.[27] The tensile strength of the electrospun nanofibrous membranes were carried out according to ASTM D5035[28] using ZWICK Z010 testing machine (ZWICK, Germany) equipped with a 100 kN load-cell at 5 mm/min and clamps distance of 15 mm. The mats with known thickness were cut into strips with dimensions of 20 mm×50 mm, mounted at the tensile tester and tested. Similarly, the tear strength of the nanofiber samples has been tested using tongue tear method (ASTM D2261).[29] The morphology of the nanofibers was characterized using FE-SEM (SEM JEOL-JSM 6390, Japan) and images were captured at an accelerating voltage of 3-10 kV for control TPU nanofibers and ABN/TPU-NFM. Energy Dispersive Spectroscopy (EDS) was used to analysis of the composition. The phase identification and crystalline stability of the ABN and ABN/TPU-NFM before and after nitrate adsorption were characterized by the XRD technique using X-ray diffractometer (XRD- 600, Shimadzu, Japan) having CuKα radiation, α = 1.54 Å with generator settings of 30 mA; 40 kV; step size 0.05 (2θ) with scan step time of 10.16 seconds in continuous mode. The FTIR spectroscopy was carried out for surface functional group

analysis using a Nicolet Avathar- 320 FTIR spectrometer (Nicolet Instruments, Madison) at a scan range of 4000-400 cm^{-1} with a scanning speed of 2 mm/sec. Leachability of the nanoparticles from the ABN/TPU-NFM has been tested using atomic absorption spectroscopy (AAS) (AA-7000 Shimadzu, Japan).

2.6. Cytotoxicity Assay

Cytotoxicity evaluation of TPU-NFM, ABN and ABN/TPU-NFM were performed using 3-(4,5-dimethylthiozol-2-yl)-2,5-diphenyl tetrazolium bromide (MTT) assay as described by Mossman.[30] Mouse fibroblast cells (L929) purchased from National Centre for Cell Science *(*NCCS), Pune, India was used. Approximately 1×10^4 mL^{-1} cells were seeded in a flat-bottomed 96-well polystyrene coated plate and were incubated for 24 h at 37° C in a 5 % CO_2 incubator. Series of dilution (0.25, 0.5, 0.75, 1.0, and 1.25 mg/mL) of sterilized ABN and different fibber sizes (2, 4, 6, 8 and 10 cm) of sterilized TPU-NFM and ABN/TPU-NFM were placed in DMEM with 5% FBS. Cells were trypsinised and seeded in a 96 well plate and desired concentration of media with ABN was added. After 24 h of incubation, 20 µL of MTT reagent was added to each well and the plates were read in a microplate reader at 570 nm. Cells without ABN were used as control.

2.7. Ground water sample collection

According to Central Ground Water Board (CGWB) report, villages in the Dharmapuri have high level of nitrate contamination in groundwater.[31] The ground water samples were collected from Nagadasampatti Village, Dharmapuri District, Tamil Nadu, India. The collected water samples were analyzed for colour, pH, TDS, F^-, NO_3^-, NH_3^+, total microbial count, salinity, resistivity, conductivity using optimized protocols. The ABN/TPU-NFM was tested for the nitrate removal from the collected ground water sample using optimized dip mode adsorption process.

3. Results and discussion

3.1. Characterization

The average membrane thickness of the developed TPU-NFM and ABN/TPU-NFM was found to be 21.7 ± 2 µm and 22.2 ± 1 µm, respectively. Similarly, the tensile strength observed for TPU-NFM and ABN/TPU-NFM was found to be 10 ± 0.2 MPa and 8 ± 0.6 MPa. The elongation at break was 207 ± 10 % and 50 ± 5 %, respectively. The tear strength of TPU-NFM and ABN/TPU-NFM was found to be 1.56 ± 0.13 N and 1.02 ± 0.07 N, respectively. As the nanofiber surface got modified with nanocomposite particles it's tensile and tear strength got reduced and it became less ductile. However, almost 80% of the strength was retained.

The control TPU nanofiber and ABN/TPU-NFM were studied using FE-SEM (Fig. 1). Fig. 1 (a) clearly indicates the formation of uniform TPU nanofibers. The control TPU nanofibers were smooth and continuous. ABN/TPU-NFM image (Fig. 1b) clearly indicate the presence of impregnated nanocomposite material on to the nanofiber. The EDS spectroscopy confirmed the composition of the ABN on the impregnated surface (Fig. 1b insert). The silane functionalization of the surface of nanocomposite as well as nanofibers facilitated uniform impregnation.

3.2. Adsorption of NO_3^- using ABN and ABN/TPU-NFM

3.2.1. Effect of contact time and initial concentration on NO_3^- adsorption

In batch mode adsorption of nitrate using ABN, the NO_3^- uptake was found to increase with time and remained constant after equilibrium. The equilibrium contact time was found to be same (60 min) for all initial NO_3^- concentrations of 25, 50, 75, 100 and 125 mg/L, respectively. The maximum NO_3^- removal was observed up to 80% in low adsorbate concentration of 25 mg/L and the percentage removal constantly reduced up to 22% as the concentration was increased to 125 mg/L (Fig. 2(a)).

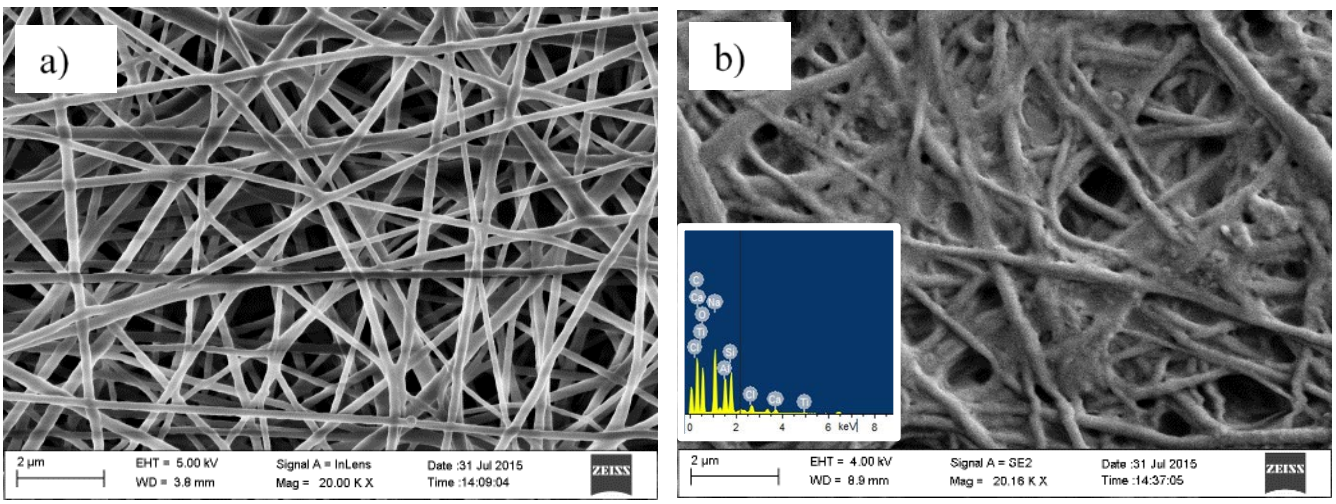

Fig. 1: FESEM images of control TPU nanofiber (a) and ABN/TPU-NFM (b) (insert: EDS Spectra of ABN/TPU-NFM)

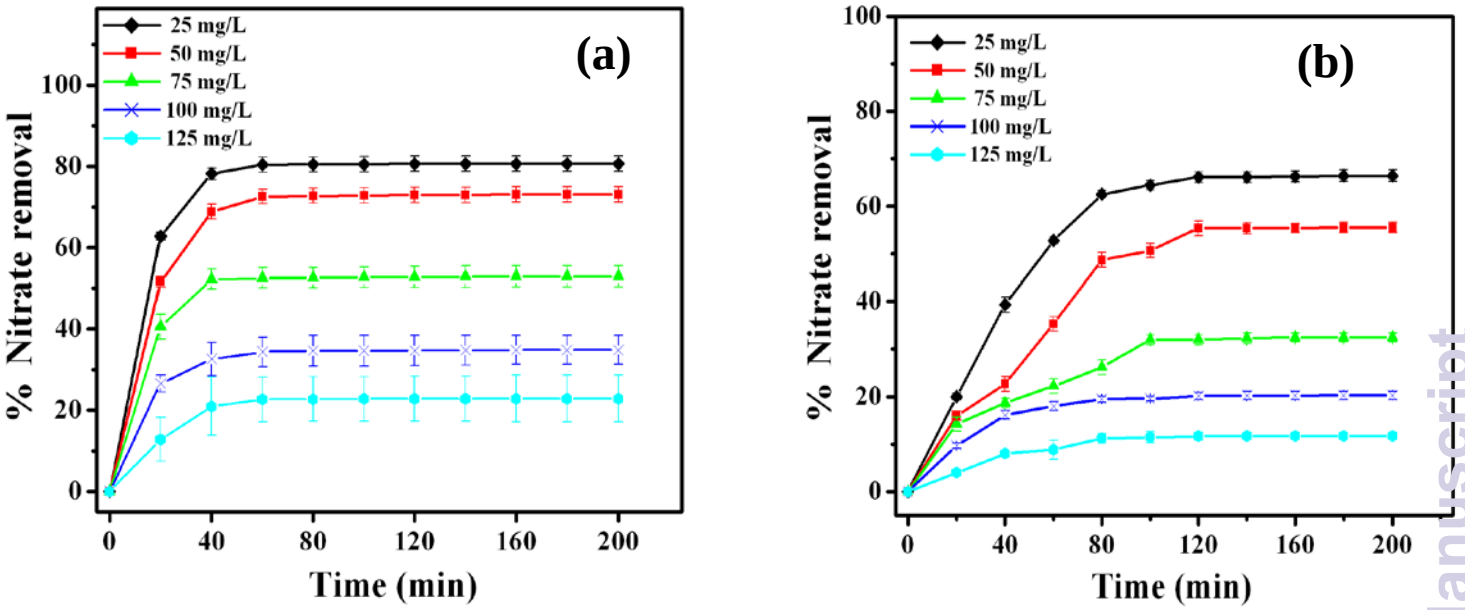

Fig. 2 Effect of contact time in the removal of nitrate using ABN (a) and ABN/TPU-NFM (b)

This showed that NO_3^- removal capacity was reduced while increasing the adsorbate concentration. The time variation curve in the NO_3^- removal capacity is smooth and continuous. Similarly, in case of dip mode adsorption studies with ABN/TPU-NFM, NO_3^- uptake was found to increase with contact time and remained constant after equilibrium. The contact time varied from 100 to 120 min as the concentration of NO_3^- increased from 25 – 125 mg/L (Fig. 2(b)). The percentage NO_3^- removal was found to be 66% for the initial NO_3^- concentration of 25 mg/L and further decreased from 66% to 12%, as the initial NO_3^-concentration increased from 25 to 125 mg/L. Similar pattern of adsorption by adsorbents have been reported earlier. The initial rapid phase of adsorption is due to the availability of a large number of active sites on the adsorbent surface[32] The change in the percentage removal is due to, initially all adsorbent sites were vacant and the solute concentration gradient was high. Hence the repulsive force between solute molecules and adsorbent phase becomes significant. Similar pattern of adsorption by adsorbents have been reported earlier. The nano-alumina prepared by Bhatnagar et al.[33] obtained maximum nitrate removal of 4 mg/g within the contact time of 15-20 min. There was no significant change in nitrate uptake by nanoalumina after 20 min. Similarly, Golestanifar et al.[34] investigated the nitrate adsorption efficiency using nanoalumina and observed the maximum adsorption efficiency of 70.8 mg/g within the contatct time of 50 min. Natural zeolite and natural zeolite-supported zero-valent iron nanoparticles showed maximum nitrate adsorption efficiency of 1.4 and 8.9 mg/g at an equilibrium contact time of about 12 and 7 h, respectively.[35]

3.2.2. Effect of ABN dosage and varying membrane size on NO_3^- adsorption

The adsorbents developed in the present study showed considerable nitrate removal and the percentage of removal varied from one adsorbent to the other. The standard nitrate solutions were treated with different dosages of ABN (0.2–1.0 g/200 mL) for equilibrium time for adsorbate concentration of 25–125 mg/L. The results revealed that increase in adsorbent dosage increased the percent removal and either reached a constant value or showed saturation after a particular dosage level. The maximum nitrate adsorption was found to be 90% of the initial nitrate concentration of 25 mg/L by increasing the ABN dosage up to 0.4 mg/200 mL and further increasing of dosage up to 1 mg/200 mL the percentage removal remains saturation. Similarly, the percentage nitrate removal decreased by increasing the initial nitrate concentration from 25 - 125 mg/L (Fig. 3 a). At lower initial nitrate concentration the adequate availability of the active sites of the nanocomposite which brings the effective adsorption. On further increase in initial nitrate concentration, the percentage removal gets decreased due to the saturation of the active sites of the constant adsorbent dosage towards the solute molecules during the adsorption. The impact of varying ABN/TPU-NFM size on NO_3^- adsorption was studied using a constant NO_3^- concentration of 75 mg/L. The pH of the solution was neutral. The results obtained are shown in Fig. 3 b. With increase in the nanofiber membrane size, the percentage NO_3^- removal was also increased from 3% to 34%.

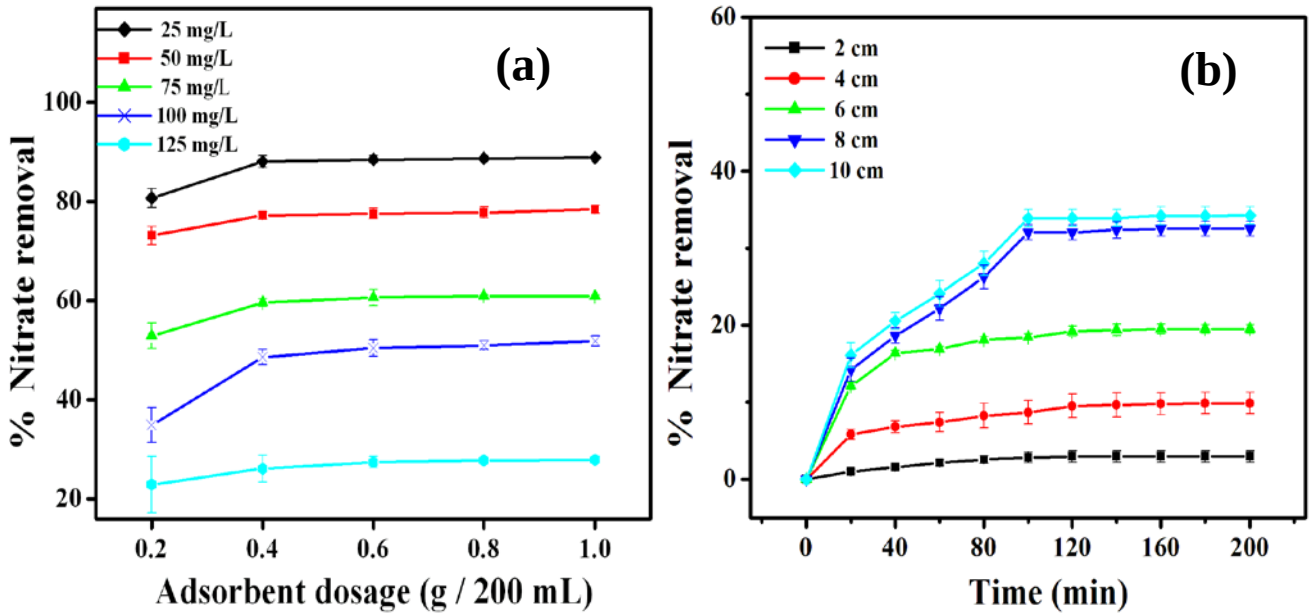

Fig. 3 Effect of adsorbent dosage using ABN (a) and varying membrane size of ABN/TPU-NFM (b) in the removal of nitrate

Table 1: First order and second order kinetics for NO_3^- adsorption by ABN and ABN/TPU-NFM

Initial NO_3^- conc. (mg/L)	q_e (exp) (mg/g)	First order kinetic model			Second order kinetic model		
		k_1 (L/ min)	q_e (cal) (mg/g)	R^2	k_2 (g/mg/min)	q_e (cal) (mg/ g)	R^2
ABN							
25	20.16	0.06	7.76	0.90	0.03	20.41	0.99
50	36.53	0.05	16.33	0.89	0.01	38.46	0.99
75	39.70	0.04	11.30	0.82	0.01	41.67	0.99
100	34.90	0.04	15.03	0.91	0.01	30.30	0.99
125	28.63	0.04	15.74	0.89	0.01	35.71	0.99
ABN/TPU-NFM							
25	16.60	0.02	8.87	0.50	0.001	19.23	0.96
50	27.77	0.03	24.37	0.61	0.000	35.71	0.91
75	24.37	0.02	14.96	0.60	0.001	27.78	0.97
100	20.27	0.02	7.88	0.49	0.004	21.74	0.99
125	14.63	0.01	5.62	0.33	0.002	16.67	0.97

The availability of more active sites and the area for the interaction of ABN on the membrane is the reason for the increase in the percent removal of the adsorbate. Similar results were observed for the adsorption of nitrate onto different adsorbent materials.[36]

3.3. Adsorption Kinetics

The rate constant of adsorption is determined from the first order rate expression given by Lagergren and Svenska.[37] The pseudo-first-order equation can be written as:

$$dq_t/dt = k_1(q_e - q_t) \quad (2)$$

Integrating this for the boundary conditions $t = 0$ to $t = t$ and $q_t = 0$ to $q_t = q_t$, gives

$$\ln (1-q_t/q_e) = -k_1 t \quad (3)$$

where k_1 is the rate constant (h^{-1}), q_e (mg/g) is the amount of solute adsorbed on the surface at equilibrium, q_t (mg/g) is the amount of solute adsorbed at any time t.
Pseudo-second-order equation (Low et al)[38] based on equilibrium adsorption can be expressed as:

$$1/q_t - 1/qe = 1/k_2 qe^2 t \quad (4)$$

Where k_2(g/mg h) is the pseudo-second-order rate constant. Both k_1 and k_2 values can be calculated from the slopes of the plots ln(1- q_t/q_e) versus t and $1/q_t$-$1/q_t$versus $1/t$, respectively.
The k_1 and k_2 values were obtained from the slopes of the plots ln (1-q_t/q_e) versus t for pseudo-first order model and $1/q_t$- $1/qe$ versus $1/t$ for pseudo-second order model, respectively. The results of fitting first order and second order kinetic model data for the NO_3^-adsorption by ABN and ABN/TPU-NFM are presented in Table 1.
The values of the coefficient of determination (R^2) clearly indicate that the experimental data are in good agreement with second order kinetic model. This may be assumed as rate-limiting step involving valence forces through sharing or exchange of electrons between the ABN on to the fibers and NO_3^- ions by chemisorption. The experimental q_e value and the calculated q_e values where matching with pseudo second order kinetic and failed to obey pseudo first order kinetics.

3.4. Adsorption isotherm

Langmuir adsorption isotherm for the NO_3^- adsorption by ABN and ABN/TPU-NFM was used to analyze equilibrium adsorption data. The isotherm is represented by the following equation (5).

$$Q_o = q_e(1 + bC_e) /bC_e \quad (5)$$

where Ce is the equilibrium concentration (mg adsorbate per litre of solution) and qe is the amount adsorbed (mg adsorbate per g of adsorbent) at equilibrium.[39] The constant Qo signifies the monolayer adsorption capacity (mg/g) and b is Langmuir constant.

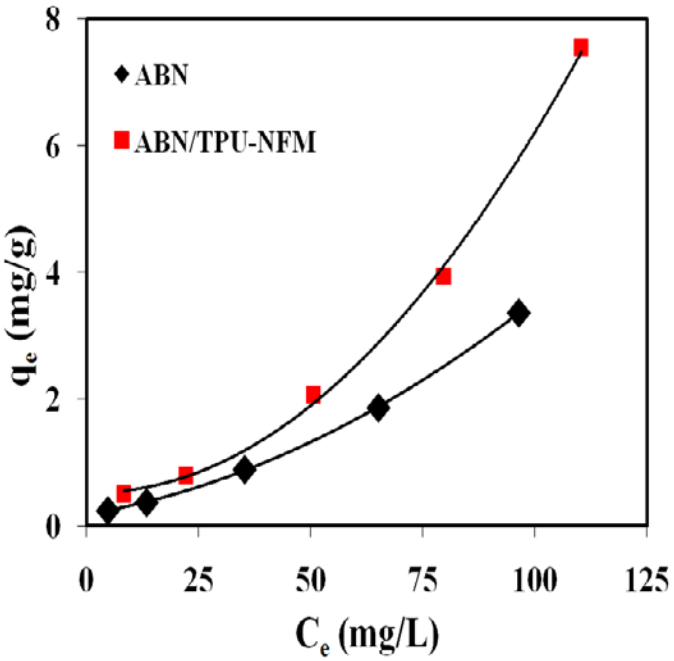

Fig. 4 Langmuir isotherm model for NO3- adsorption by ABN and ABN/TPU-NFM

Plots of qe vs. Ce show the agreement of experimental data with Langmuir plot for NO_3^- removal using synthesized adsorbent materials (Fig. 4). The maximum NO_3 adsorption capacity (Q_o) of the ABN and ABN/TPU-NFM adsorbent materials was found to be 30.3 and 14.9 mg/g, respectively. The NO_3^- adsorption capacity of the adsorbents developed in the present study was higher than that of the other reported values in literature (Table 2).

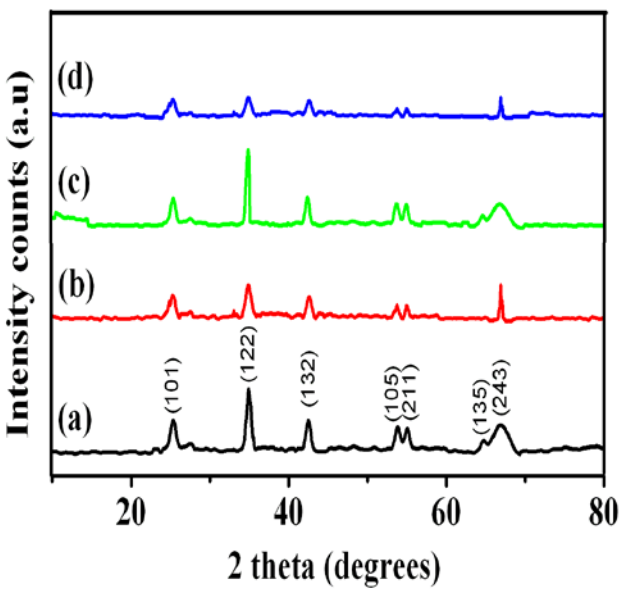

Fig. 5 XRD pattern of ABN and ABN/TPU-NFM before (a,b) and after (c,d) nitrate adsorption.

Table 2: Summary of the maximum NO_3^- removal capacities by different adsorbents

S. No	Adsorbents	Adsorption capacity (mg/g)	Ref
1.	Activated carbon	5.8	[40]
2.	Zcl_2 activated carbon	10.3	[41]
3.	cetylpyridinium bromide (CPB) modified zeolite	9.68	[42]
4.	hexadecyltrimethyl ammonium (HDTMA) modified zeolite	11.4	[43]
5.	Activated sepiolite	9.8	[44]
6.	granular chitosan-Fe^{3+} complex	8.35	[45]
7.	hexadecyltrimethylammonium bromide modified (hdtma) bentonite	12.83	[46]
8.	hydrous bismuth oxides HBO_3	0.22	[47]
9.	quaternary (polypropylene-g-N,N-dimethylamino ethylmethacrylate) graft copolymer,	12.5	[48]
10.	Nano-alumina	4.0	[33]
11.	polyacrylonitrile coated with iron oxide nano particles	2.09	[49]
12.	Ion-exchange polyHIPE type membrane	27.03	[50]
13.	cationic polymer-modified granular activated carbon	26	[51]
14.	ABN	30.3	Present study
15.	ABN/TPU-NFM	14.9	Present study

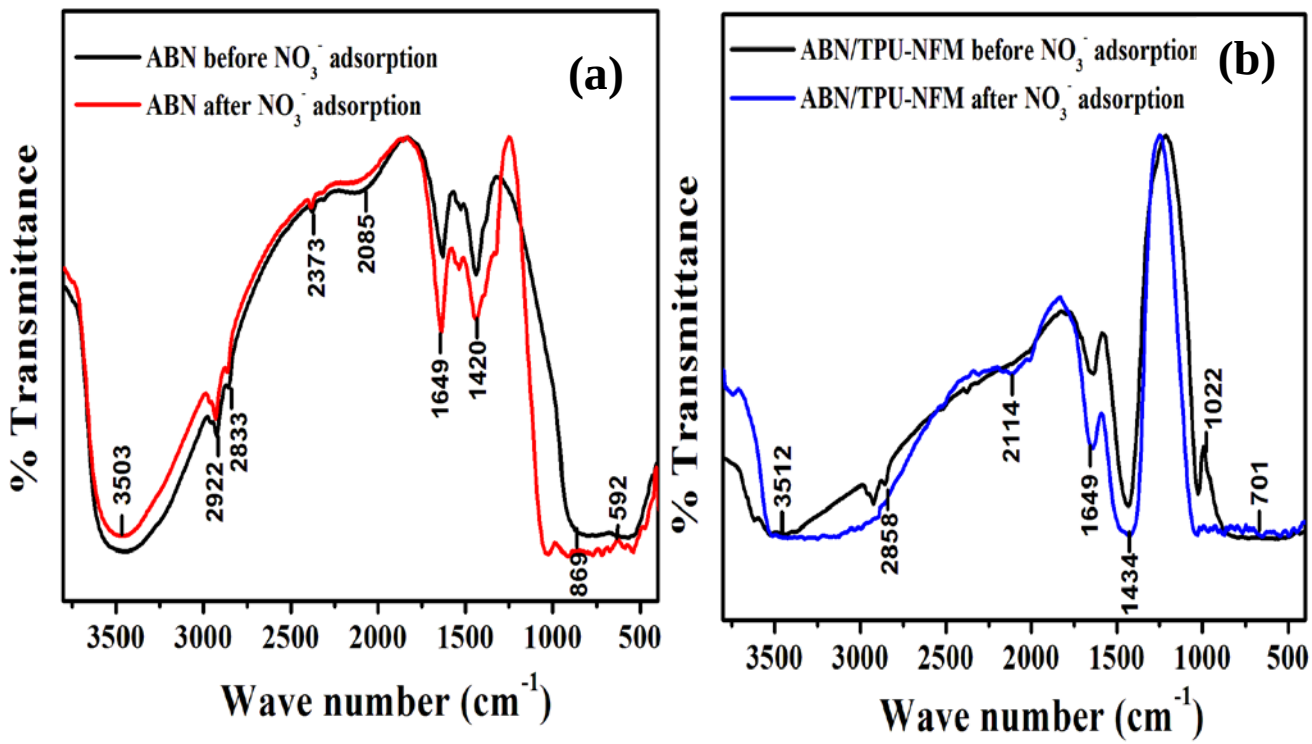

Fig. 6 FTIR spectrum of ABN (a) and ABN/TPU-NFM (b) before and after nitrate adsorption.

3.5. ABN and ABN/TPU-NFM before and after nitrate adsorption

ABN and ABN/TPU-NFM were studied using XRD and FTIR spectroscopy before and after nitrate adsorption. The phase identification and crystal structure data of the ABN AND ABN/TPU-NFM were already reported in our previous paper.[22] In brief, the intensity peaks (122, 132 and 243) corresponded to the orthorhombic crystal structure of alumina, the intensity peaks (101, 105 and 211) corresponded to anatase phase having body centred tetragonal crystal structure of titania in the adsorbent materials. The ABN and ABN/TPU-NFM after nitrate adsorption clearly shows that the materials have high crystalline stability (Fig. 5). The crystalline nature of adsorbent has not been changed even after react with nitrate ions. The adsorption mainly occurs on the surface oxide groups of the nanocomposite thus it does not have any impact on the crystallinty of the nanocomposite. The FTIR spectra (Fig. 6 (a, b)) of the ABN and ABN/TPU-NFM showed a characteristic bands at 3503 and 3512 cm^{-1}, which was assigned to the surface OH group. The bands at 2922, 2833 and 2858 cm^{-1} can be attributed to the asymmetric and symmetric stretching of CH_2 group. The atmospheric CO_2 asymmetrical stretching vibration resulted in characteristic bands at 2373, 2085 and 2114 cm^{-1}. [52,53] The FTIR spectra show that the functional hydroxyl groups were involved in the adsorption reaction, and a band shift from 869 and 1022 cm^{-1} to 592 and 701 cm^{-1} was observed (Fig. 6 (a, b)). Such a band shift is due to the hydroxide bridging between nitrate ions and the metal oxide surfaces. The intensity of the O–H band decreases after NO_3^- adsorption and this showed that the surface hydroxyl groups of the nanocomposite present on the nanofibers were involved in the NO_3^- adsorption.[33] Similar observations have been reported by various researchers.[52,53] The adsorption of nitrate onto nanocomposite adsorbent used in the present study can be explained by the formation of surface complexes according to the schematic representation (Fig. 7). The extent of adsorption is limited to the number of exchangeable surface hydroxyl groups, which is a function of surface area.[24] Hence, the nitrate adsorption by ABN nanocomposite using batch process showed better nitrate adsorption than dip mode adsorption of ABN/TPU-NFM. The percent removal is more with free ABN when compared to the ABN/TPU-NFM because the available surface area, active site and the reactivity of ABN decreases with adherence/attachment to nanofiber. Since the nanofiber does not contribute to nitrate removal and merely acts as a substrate for ABN attachment, the activity of ABN is more in free form than the ABN that is fixed to membrane.

3.5. Leachability and toxicity analysis

The leachability studies using AAS showed no significant leaching of alumina or titania from nanocomposite impregnated nanofibers during the adsorption process. This result indicates that the nanocomposite particles have bound strongly to the nanofiber. The cytotoxicity effect of ABN, TPU-NFM and ABN/TPU-NFM towards the mouse fibroblast cells (L929) was studied using MTT assay. The viability percentage of ABN treated cells at different concentrations (0.25, 0.5, 0.75, 1.0, and 1.25 mg/mL) is given in Fig. 8 (a). ABN was found to be nontoxic and showed good proliferation with L929 cells in all concentration (>70% viability). Similarly, the different sizes of (2 to 10 cm) TPU-NFM and ABN/TPU-NFM showed good proliferation towards L929 cells (>65% viability) (Fig. 8 (b and c)).

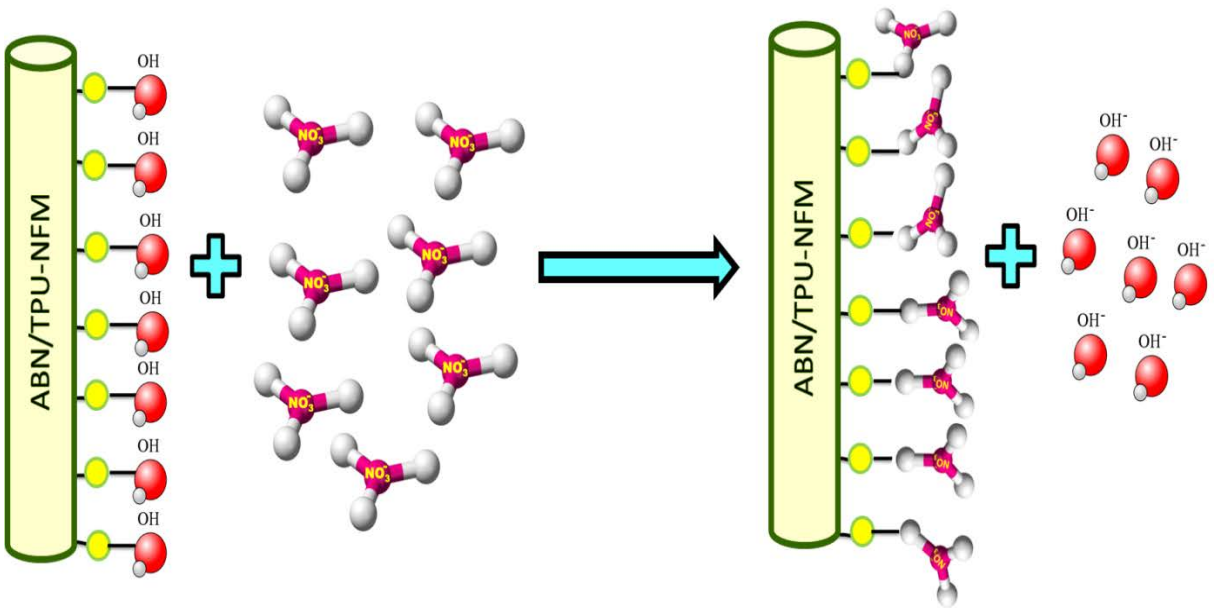

Fig. 7 Schematic representation of mechanism of nitrate adsorption by ABN/TPU-NFM

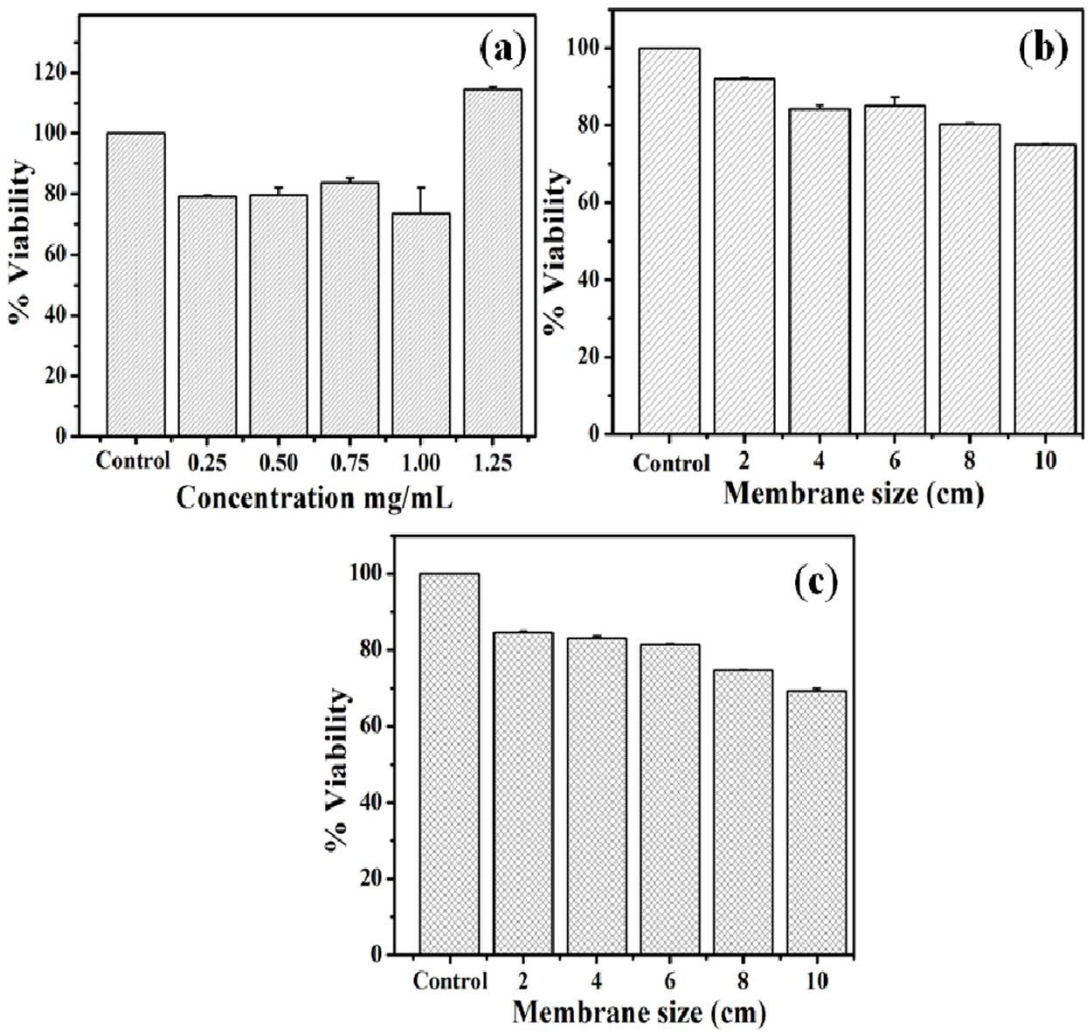

Fig. 8 Toxicity study of ABN (a) TPU-NFM (b) and ABN/TPU-NFM (c) using Mouse fibroblast cells (L929)

As the TPU-NFM and ABN/TPU-NFM membrane area was increased there was slight decrease in the viability of cells. This may be due to the adaptability of the cells to the new nanocomposite surface. The above results clearly indicated that the developed nanocomposite and nanocomposite impregnated nanofibrous membrane were nontoxic, biocompatible and can be used for water purification systems. Qiang et al.[54] reported 70% of viability at 0.25 mg/mL TiO_2 and above 70 % viability for (0.25-1.25 mg/mL) of Al_2O_3 on human fibroblast cell. In our study, the nanocomposite impregnated membrane containing both TiO_2 and Al_2O_3 was found to show similar nontoxic activity.

3.6. Nitrate removal from natural groundwater sample

The natural ground water sample was analyzed for initial parameters and subjected to dip mode adsorption using ABN/TPU-NFM (8x8 cm^2) for 120 min. The collected ground water sample had 86 ±1 mg/L of nitrate concentration. The ground drinking water also contained other contaminants like fluoride, ammonia and high total dissolved solids (TDS) above their permissible level. The water pollutant levels before and after adsorption is shown in Table 3. These results suggested that the ABN/TPU-NFM effectively removes nitrate ions from ground water sample without altering the pH along with other contaminants. The nitrate concentration in the sample reduces up to 31.7±0.58 mg/L which is well below its maximum contamination level. The ABN/TPU-NFM also have the ability to reduce the fluoride level within permissible limit which correlates with our previous work on fluoride adsorption using the above adsorbent.[24] The changes in other pollutants were listed in the Table 3.

Table 3: Change in the pollutants before and after dip mode adsorption using ABN/TPU-NFM towards natural ground water

Sr. No	Parameters (units)	Before treatment	After treatment	Permissible limit[5]
1.	Visibility & nature	Clear	Clear	Clear
2.	Odour	no	no	Unobjectionable
3.	pH	7.44 ± 0.05	7.21 ± 0.02	6.5 to 8.5
4.	Nitrate (mg/L)	86 ± 1	31.7 ± 0.58	50
5.	Fluoride (mg/L)	3.6 ± 0.17	0.4 ±0.006	1.0
6.	Ammonia (mg/L)	0.03 ± 0.002	0.01 ± 0.003	0.5
7.	Total dissolved solids (mg/L)	1778 ± 19.1	1686 ± 4.7	500
8.	Salinity (mg/L)	1752 ± 16.8	1572 ± 2.9	600
9.	Resistivity (Ω)	170 ± 1.7	191 ± 1.5	-
10.	Conductivity (Ms)	3.13 ± 0.06	2.82 ± 0.07	2
11.	Total bacterial count (CFU/mL)	25 ± 2	16 ± 3	No relaxation

4. Conclusions

The developed adsorbent materials were successfully studied for the efficient removal of nitrates from water using both batch and dip mode adsorption process. The maximum adsorption capacity (Q_0) of the ABN and ABN/TPU-NFM adsorbents was found to be 30.3 and 14.9 mg/g. The adsorption kinetic process obeys pseudo second order kinetic and failed to obey pseudo first order kinetic models. The leachability studies revealed that the developed nanocomposite did not leach from the membrane. The Nanocomposite was found to be non toxic suggesting that the developed hybrid adsorbent is biocompatible and safe for use in purification of drinking water. The ABN/TPU-NFM was tested towards the natural ground water and showed that the adsorbent material can bring down the nitrate concentration below the maximum permissible limit in drinking water. The developed nanomposite impregnated membrane (ABN/TPU-NFM) is easy to use through a simple dipping process as compared to other reported techniques.

Acknowledgment

The authors are thankful to Life Science Research Board (DRDO-LSRB) (Sanction no: LSRB-235/BTB/2011), Govt of India, for funding this study. Support and help rendered by PSG Management and PSG Institute of Advanced Studies is acknowledged. The authors are thankful to Bayer Material Science for providing polymers.

Notes and references

[a]Nanobiotechnology laboratory, PSG Institute of Advanced Studies, P.B. No: 1609, Peelamedu, Coimbatore 641004, India. Tel.: +91 422 4344000 extn 4327; E-mail: selvabiotech@gmail.com, *rsk@psgias.ac.in*

[b] Tissue Engineering laboratory, PSG Institute of Advanced Studies, P.B. No: 1609, Peelamedu, Coimbatore 641004, India.

[c] Advanced Textile and Polymer Research Laboratory, Nanotech Research Facility, PSG Institute of Advanced Studies, Peelamedu, Coimbatore 641004, India

1. M. Kumar and A. Puri, *Indian J. Occup. Environ. Med.*, 2012, **16**, 40.
2. S. P. Suriyaraj, B. M. Benasir, S. G. Deepika, P. Biji and R. Selvakumar, *Water Sci. & Tech.: Water Supp.*, 2014, **14**, 554.
3. B. C. Kross, *J. Prevent. Med.*, 2002, **10**, 3.
4. K. Brindha, R. Rajesh, R. Murugan and L. Elango, *Appl. Geochem.*, 2010, **12**, 231.
5. WHO, Guidelines for Drinking- water Quality. fourth ed. World Health Organisation, 2011
6. K. Y Cheng, A. H Kaksonen, G. B Douglas. *Bioresour Technol.*, 2014, **172**, 373.
7. E. Lacasa, P. Cañizares, C. Sáez, F. J. Fernández , M. A. Rodrigo, *Chem. Eng.* 2011,**171**,1012.
8. J.J. Schoeman, A. Steyn, *Desalin.*, 2003, **155**, 15.
9. L. Banasiak and A. Schafer(2009) *J. Membr. Sci.*, 2009, **334**, 101.
10. N. Ozturk and T. E. Bektas, *J. Hazard. Mater.*, B. 2004, **112**, 155.
11. R. Mukherjee and S. De, *J. Memb. Sci.*, 2014, **466**, 281.
12. A. Bhatnagar and M. Sillanpaa, *Chem. Eng.*, 2011, **168**, 493.
13. Halajnia, S. Oustan, N. Najafi, A. R. Khataee and A. Lakzian, *Appl. Clay Sci.*, 2012, **70**, 28.
14. M. Islam and R. Patel, *J. Hazard. Mater.*, 2011, **190**, 659.
15. W. Gao, J. Chen, X. Guan, R. Jin, F. Zhang and N. Guan, *Catal. Today*, 2004, **93**, 333.
16. J. A. Anderson, *Catal. Today*, 2011, **175**, 316.
17. S. Jung, S. Bae and W. Le, *Environ Sci Technol.*, 2014, **48**, 9651.
18. S. Ambonguilat, H. Gallard, A. Garron, F. Epron and J. P. Croue, *Water Res.*, 2006, **40**, 675.
19. Z. Gao, Y. Zhang, D. Li, C. J. Werth, Y. Zhang and X. Zhou, *J. Hazard. Mater.*, 2015, **3**, 425.
20. M. S. Kim, S. H. Chung, C. J. Yoo, M. S. Lee, I. H. Cho and D. W. Lee, *Appl. Catalysis B: Env.*, 2013, **142**, 354.
21. S. Witonska, J. Karski and J. K. Gołuchowska, *Kinet. Catal.*, 2007, **48**, 823.

22. A. Navrotsky, Environmental nanoparticles. In: Dekker Encyclopedia of Nanoscience and Nanotechnology, J.A. Schwarz, C. Contescu, K. Putyera (Eds). 2004, **2**, 1147.
23. L. Srivastav, P. K. Singh, V. Srivastava and C. Y. Sharma, *J. Hazard. Mater.*, 2013, **263**, 342.
24. S. P. Suriyaraj, A. Bhattacharyya and R. Selvakumar, *RSC Adv.*, 2015, **5**, 26905.
25. S. P. Suriyaraj and R. Selvakumar, RSC Adv., 2014, **4**, 39619.
26. www.epa.gov/solidwaste/hazard/testmethods/sw846/pdfs/**9210** a.pdf
27. http://www.astm.org/Standards/D1777.htm
28. http://www.astm.org/Standards/D5035.htm
29. http://www.astm.org/Standards/D2261.htm
30. T. Mosmann, *J. Immuno. Meth.*, 1983, **65**, 55.
31. CGWB (2009) District groundwater brochure Dharmapuri District, Tamil Nadu. Technical Report series, cgwb.gov.in/District_Profile/TamilNadu/Dharmapuri.pdf
32. M. A. Jaworski, I. D. Lick, G. J. Siri and M. L. Casella, *Appl. Catalysis B: Env.*, 2014, **156**, 53.
33. A. Bhatnagar, E. Kumar, M. Sillanpaa, *Chem. Eng. J.*, 2010, **163**, 317.
34. H. Golestanifar, A. Asadi, A. Alinezhad, B. Haybati and M. Vosoughi, *Desalin. Water Treat.*, 2015, 1.
35. S. Sepehri, M. Heidarpour and J. Abedi-Koupai, *Soil & Water Res.*, 2014, **9**, 224.
36. N. Oztürk and T. E. Bektaş, *J Hazard Mater., 2004*, **112**, 155.
37. S. Lagergren and B. K. Svenska, *Vetenskapsakad. Handl.*, 1898, 24, 1.
38. L. W. Low, T. T. Teng, A. Ahmad, N. Morad, Y. S. Wong, *Water, Air, & Soil Pollution*, 2011,**218**, 293.
39. Langmuir, *J. Am. Chem. Soc.*, 1918, **40**, 1361.
40. H. J. Park and C. K. Na, *J. Colloid Interf. Sci.*, 2006, **301**, 46.
41. Namashivyam and D. Sangeetha, *Indian J Chem. Techn.*, 2005, **12**, 513.
42. Y. Zhan, J. Lin and Z. Zhua, *J. Hazard. Mater.*, 2011, **186**, 1972.
43. M. S. Onyango, M. Masukume, A. Ochieng and F. Otieno, *Water SA*, Vol. 2010, 36.
44. N. Ozturka and T. E. Bektas, *J. Hazard. Mater.*, B, 2004, **112**, 155.
45. Q. Hu, N. Chen, C. Feng and W. W. Hu, *Appl. Surf. Sci.*, 2015 In Press, Accepted Manuscript .
46. Y. Xi, M. Mallavarapu and R. Naidu, *Appl. Clay Sci.*, 2010, **48**, 92.
47. P. K. Singh, S. Banerjee, A. L. Srivastava and Y. C. Sharma, *RSC Adv.*, 2015, **5**, 35365.
48. M. F. A. Taleb, G. A. Mahmoud, S. M. Elsigeny, E. S. A Hegazy, *J. Hazard. Mater.*, 2008, **159**, 372.
49. R. Nabizadeh, M. Jahangiri-rad and M. Rafiee, *Res. J. Environ. Sci.*, 2014, **8**, 287.
50. M. Alikhani and M. R. Moghbeli, *Chem. Eng. J.*, 2014, **239**, 93.
51. W. Cho, C. M. Chon, Y. Kim, B. H. Jeona, F. W. Schwartzc and E. S. Leed, *Chem. Eng. J.*, 2011, **175**, 298.
52. P. A. Patel, J. Eckart, M. C. Advincula, A. J. Goldberg and P. T. Mather, *Polymer*, 2009, **50**, 1214.
53. S. Devaraju, P. Prabunathan, M. Selvi and M. Alagar, *Front Chem.*, 2013, **1**, 19.
54. Z. X. Qiang, Y. L. Hong, T. Meng and P. Y. Pu, *Biomed Environ Sci.*, 2011, **24**, 661.